Published in final edited form as:
Cell Motil Cytoskeleton. 2008 December ; 65(12): 945–954. doi:10.1002/cm.20317.

Expression and Alternative Splicing of N-RAP during Mouse Skeletal Muscle Development

Shajia Lu[*], **Diane E. Borst**[+], and **Robert Horowits**[*]

[*]Laboratory of Muscle Biology, National Institute of Arthritis and Musculoskeletal and Skin Diseases, National Institutes of Health, Department of Health and Human Services, Bethesda, MD 20892

[+]Department of Anatomy, Physiology and Genetics, Uniformed Services University of the Health Sciences, Bethesda, MD 20814

Abstract

N-RAP alternative splicing and protein localization were studied in developing skeletal muscle tissue from pre- and postnatal mice and in fusing primary myotubes in culture. Messages encoding N-RAP-s and N-RAP-c, the predominant isoforms of N-RAP detected in adult skeletal muscle and heart, respectively, were present in a 5:1 ratio in skeletal muscle isolated from E16.5 embryos. N-RAP-s mRNA levels increased three-fold over the first three weeks of postnatal development, while N-RAP-c mRNA levels remained low. N-RAP alternative splicing during myotube differentiation in culture was similar to the pattern observed in embryonic and neonatal muscle, with N-RAP-s expression increasing and N-RAP-c mRNA levels remaining low. In both developing skeletal muscle and cultured myotubes, N-RAP protein was primarily associated with developing myofibrillar structures containing α-actinin, but was not present in mature myofibrils. The results establish that N-RAP-s is the predominant spliced form of N-RAP present throughout skeletal muscle development.

Keywords

myofibrillogenesis; myotube; sarcomere

Introduction

N-RAP is a striated muscle-specific scaffolding protein involved in myofibril assembly (Luo et al., 1997; Carroll et al., 2001; Carroll et al., 2004; Dhume et al., 2006). The N-RAP gene is highly conserved between mouse and humans, and consists of 42 exons spread over 70 kilobases (Mohiddin et al., 2003). These exons encode a 196 kilodalton protein consisting of an N-terminal LIM domain, 11 modules homologous to single nebulin repeats, and an additional 35 modules arranged into 5 super repeats homologous to nebulin super repeats. A single 35 amino acid nebulin-like repeat encoded by exon 12 is alternatively spliced (Mohiddin et al., 2003; Gehmlich et al., 2004). The N-RAP isoform including exon 12 predominates in adult skeletal muscle but is not expressed in cardiac muscle, leading us to term the isoform containing this exon N-RAP-s and the isoform lacking this exon N-RAP-c (Mohiddin et al., 2003). Alternative splicing of N-RAP exon 39 has also been reported in human skeletal muscle (Gehmlich et al., 2004).

Address for Correspondence: Dr. Robert Horowits, Building 50, Room 1154, MSC 8024, National Institutes of Health, Bethesda, MD 20892-8024, Telephone: 301-435-8371, horowits@helix.nih.gov.

Myofibril assembly has been the subject of much research, leading to several models describing the specific sequence of events by which linear arrays of sarcomeres are assembled from actin filaments, myosin filaments, and titin filaments (Gregorio and Antin, 2000; Sanger et al., 2005). The earliest myofibril precursors containing punctate α-actinin Z-bodies, α-actin and muscle tropomyosin appear near the cell periphery as immature fibrils (Dlugosz et al., 1984; Wang et al., 1988; Schultheiss et al., 1990; Handel et al., 1991; Rhee et al., 1994; Dabiri et al., 1997; Imanaka-Yoshida, 1997; Ehler et al., 1999; Rudy et al., 2001; Lu et al., 2005). Nonmuscle myosin IIB is also present between the Z-bodies of premyofibrils and and the Z-lines of nascent sarcomeres, but is gradually replaced by muscle myosin filaments (Rhee et al., 1994) that are assembled separately (Holtzer et al., 1997; Srikakulam and Winkelmann, 2004).

In addition to nonmuscle myosin IIB, scaffolding proteins such as N-RAP and Krp1 are transiently associated with myofibril precursors during assembly (Carroll and Horowits, 2000; Lu et al., 2003; Lu et al., 2005; Greenberg et al., 2008). N-RAP binds many cytoskeletal proteins in vitro, including talin, vinculin, filamin, α-actinin, and actin (Luo et al., 1999; Lu et al., 2003), consistent with a scaffolding function for this protein. A role for N-RAP in myofibril assembly is supported by cell biological studies in cultured cardiomyocytes demonstrating that N-RAP domains expressed as GFP fusion proteins interfere with myofibril assembly (Carroll et al., 2001; Carroll et al., 2004) and that N-RAP knockdown by RNA interference halts myofibril assembly (Dhume et al., 2006). A molecular mechanism by which N-RAP scaffolds α-actinin and actin assembly into symmetrical I-Z-I structures has been proposed (Carroll et al., 2001; Carroll et al., 2004).

Here we observe N-RAP alternative splicing and localization in developing embryonic and neonatal skeletal muscle as well as in differentiating myotubes in culture. The results confirm the association of N-RAP with developing myofibrillar structures as previously observed in cardiomyocytes, and establish that N-RAP-s is the predominant spliced form of N-RAP present throughout skeletal muscle development.

Materials and Methods

Animals

Timed pregnant CD-1 mice were purchased from Charles River Laboratories (Wilmington, MA) and used for muscle tissue studies. SJL/J mice were purchased from The Jackson Laboratory (Bar Harbor, Maine) and used to prepare primary cultures of skeletal muscle. All animal handling procedures were performed under a National Institutes of Health animal study proposal approved by the NIAMS Animal Care and Use Committee.

Primary Culture of Mouse Skeletal Muscle

The muscles were excised from the lower limbs of 5 week-old SJL/J mice, thoroughly minced, and digested in 0.2% type II collagenase (Worthington Biochemicals, Lakewood, NJ) in DPBS buffer with calcium (Invitrogen, Carlsbad, CA) for 30 minutes at 37 °C. After digestion the cells were collected via a 5 minute centrifugation at 1800g. The collected cells were exposed to 1× trypsin-EDTA (0.25% with 1 mm EDTA from Invitrogen) at 37 °C for 10 minutes. The cells were diluted in 30 ml of culture medium containing 10% horse serum (Invitrogen), 20% FBC (Invitrogen), 1% chick embryo extract (US Biological, Swampscott, MA), and 1% penicillin-streptomycin (Invitrogen) in DMEM (Invitrogen) and filtered through 40 μm cell strainers (BD Biosciences, Bedford, MA). Fibroblasts adhere to uncoated culture dishes more readily than muscle cells (Sanger et al., 2002), so fibroblast contamination was minimized by pre-plating the cells onto 100-mm tissue culture dishes overnight at 37 °C. The unattached cells were centrifuged at 1800g for 5 minutes, suspended in culture medium, plated onto dishes coated with matrigel (BD Biosciences) and incubated at 37 °C overnight. The attached cells

were trypsinized, suspended in culture medium and plated at 1-2 × 10^5 cells/ml on 0.25% laminin (Invitrogen) coated tissue culture dishes or glass-bottom cover slides. After one day in culture, the culture medium was replaced with differentiation medium containing 2% horse serum, 1× insulin-transferrin-selenium, and 1% penicillin-streptomycin in DMEM (Invitrogen).

RNA Isolation and RT-PCR

The PCR primers used for semi-quantitative RT-PCR analysis of isolated muscle and quantitative real-time PCR analysis of cultured muscle are defined in table 1. Total RNA was isolated from tissue and mRNA levels were analyzed by semi-quantitative RT-PCR as previously described (Lu et al., 2005). For analysis of gene expression in primary cultured skeletal muscle cells, total RNA was extracted and purified using the RNeasy Mini Kit (Qiagen, Valencia, CA) according to the manufacturer's instructions. First-strand cDNA was synthesized using 0.2 μg of total RNA and random hexamer primers in a 20 μl reverse transcriptase reaction mixture (BD Biosciences Clontech, Palo Alto, CA) as per the manufacturer's instruction. Real-Time PCR reactions were performed using an MX3000p Real-Time PCR unit (Stratagene, Cedar Creek, TX) with SYBR Green detection. Each sample was amplified in a 50 μl mixture containing 0.2 μl cDNA, 400 nM of each primer, and ROX as the reference dye. The PCR cycle conditions were 95 °C for 10 minutes; followed by 40 cycles at 95 °C for 5 seconds, then 60 °C for 1 minute; followed by 72 °C for 1 minute. Accumulation of the amplified target was monitored during the early exponential phase of the amplification process. 18s rRNA was amplified using QuantumRNA 18s Universal Internal Standard primers (Ambion, Austin, TX) and was used as an internal control to normalize the amplification of target genes. To distinguish between fluorescence derived from specific and non-specific products, SYBR green dye-based QPCR assays included dissociation curves for each gene analyzed. The data were analyzed using the comparative C_T method (Giulietti et al., 2001;Livak and Schmittgen, 2001). Using the relative quantitation method requires that the PCR efficiencies of all genes be similar and preferably at or above 90%. A standard curve of serial dilutions of templates for each gene was tested and amplification efficiencies ranged from 94-103%.

Immunofluorescence Staining and Microscopy

Mouse embryos were fixed, frozen, sectioned, and stained as previously described (Lu et al., 2005). Stained embryo sections were visualized using a Zeiss Axiovert 135 microscope and the micrographs were processed to remove background and out of focus fluorescence by digital deconvolution using IPLab (Scanalytics, Fairfax, VA) and MicroTome (VayTek, Fairfield, IA) software, as previously described (Lu et al., 2005). Sections exposed to N-RAP antibody and nonimmune control serum were captured and processed identically for comparison.

Primary skeletal muscle cultures were fixed at varying times with 4% formaldehyde (Ted Pella, Redding, CA) in phosphate buffered saline (PBS), and then permeated with 0.1% Nonidet-P-40 in PBS. Cells were blocked with 5% goat serum (Sigma-Aldrich, St. Louis, MO) in PBS for 30 min. Then the cell cultures were exposed to a polyclonal antibody against N-RAP (Luo et al., 1997) at a dilution of 1:1000. The N-RAP antibody was detected using an Alexa Fluor 488-linked secondary antibody (goat anti-rabbit IgG; Molecular Probes, Eugene, OR) at a dilution of 1:500. Cells were then exposed to a monoclonal antibody against sarcomeric α-actinin (clone EA-53 from Sigma-Aldrich) at a dilution of 1:2000 followed by detection using a rhodamine-linked rabbit anti-mouse secondary antibody at a dilution of 1:1000 (Sigma-Aldrich). All antibody dilutions were in PBS and all antibody incubations were at 37 °C for 1 hour. To prevent photobleaching, Vectashield (Vector Laboratories, Burlingame, CA) was added to each well. Stained cultured cells were imaged with a Zeiss LSM 510 Meta laser

scanning confocal microscope (Carl Zeiss, Thornwood, NY) using 63×/1.4 oil or 10× objectives.

Results

N-RAP Expression and Alternative Splicing During Muscle Development

We used semi-quantitative RT-PCR to investigate N-RAP expression levels and alternative splicing during skeletal muscle development. Primers were designed to amplify exons 9-14 of the N-RAP message, which includes the alternatively spliced exon 12, as well as exons 36-41, in which no alternative splicing has been detected (figure 1A). We found that total N-RAP expression increased steadily from E16.5 to postnatal day 21 (figure 1B), but that α-actinin mRNA levels remained constant during this period (data not shown). The increase in N-RAP mRNA was entirely due to increasing levels of the N-RAP-s isoform, which contains exon 12 (figure 1C-D). Low levels of N-RAP-c, the splice varient without exon 12, were also detected in skeletal muscle, but N-RAP-c expression was five-fold lower than N-RAP-s at E16.5 and did not subsequently increase. In contrast, only N-RAP-c was expressed in mouse heart (figure 1C and (Lu et al., 2005)).

Figure 2 shows skeletal muscle-containing regions of sectioned E14.5 embryos labeled with antibodies against sarcomeric α-actinin and N-RAP. The large area marked by an asterisk in panels A-C contains cells detected by nuclear Dapi staining that were unlabeled by either of the antibodies, illustrating the muscle-specificity of these reagents. At higher magnification, N-RAP staining was clearly associated with developing myofibrils marked by punctate dots of α-actinin (figure 2A-F, arrows). In more mature but still narrow striations containing α-actinin, N-RAP staining was present at twice the periodicity of the nascent Z-lines (figure 2A-F, arrowheads).

By E17.5 the skeletal muscles were typically filled with long stretches of mature myofibrils. Figure 3 shows a myotendinous junction region from an E17.5 embryo labeled with antibodies against sarcomeric α-actinin and N-RAP. The α-actinin is organized into broad-banded Z-lines, and N-RAP is nearly all concentrated at the myotendinous junction region of the muscle cells.

N-RAP Expression and Alternative Splicing in Cultured Myotubes

Primary skeletal muscle cultures initially consisted of mononucleated myoblasts expressing very low levels of sarcomeric α-actinin and N-RAP, proteins specifically found in differentiated muscle (figure 4, left panel). Serum withdrawal promoted myoblast fusion to form differentiated myotubes containing α-actinin and N-RAP (figure 4). We used real-time PCR to quantitate mRNA levels of muscle-specific genes during myoblast differentiation and fusion in culture. PCR primer pairs were designed to specifically amplify regions of N-RAP-s and total N-RAP messages (figure 5A). Total N-RAP and Krp1, scaffolding proteins that promote distinct steps in myofibril assembly (Carroll et al., 2001;Carroll et al., 2004;Greenberg et al., 2008), were expressed within one day of culture in differentiating medium and continued increasing over several days. In contrast, sarcomeric α-actinin expression remained low after one day and then rapidly increased over the subsequent two days (figure 5B). The increase in N-RAP expression was approximately equally divided between the two N-RAP isoforms over the first two days, after which N-RAP-s continued to increase while N-RAP-c decreased to undetectable levels (figure 5C).

Figure 6 shows cultured myotubes stained with antibodies against sarcomeric α-actinin and N-RAP. N-RAP was most often associated with closely spaced dots of α-actinin (figure 6). In some cases N-RAP appeared organized as punctate linear arrays associated with long arrays of periodic dotted α-actinin staining (figure 6A-F, brackets). In other cells N-RAP staining was

organized as patches associated with shorter regions of dotted α-actinin (figure 6G-I). N-RAP was not detected in regions containing mature Z-lines (figure 6G-I, asterisks) or at the spreading lateral edge of the myotubes (figure 6D-F, arrow).

Discussion

N-RAP & Myofibril Assembly

The evidence supporting a role for N-RAP as a scaffolding protein in myofibril assembly is based on localization, expression, and knockdown studies in developing heart tissue and cultured cardiomyocytes (Carroll and Horowits, 2000; Carroll et al., 2001; Carroll et al., 2004; Lu et al., 2005; Dhume et al., 2006). Here we observe that N-RAP is associated with punctate patterns of α-actinin staining that are characteristic of premyofibrils in both developing skeletal muscle from embryos as well as in cultured myotubes (figures 2 and 6). Furthermore, N-RAP expression increases during skeletal muscle development in vivo (figure 1), and levels of mRNAs encoding N-RAP and Krp1 both increase before α-actinin expression during myoblast fusion and differentiation in culture (figure 5B). N-RAP and Krp1 are both scaffolding proteins that promote distinct steps in myofibril assembly (Greenberg et al., 2008), and these data suggest that during muscle differentiation genes encoding assembly scaffolds are activated before genes encoding structural components of myofibrils. Interestingly, N-RAP levels continued increasing during cardiac (Lu et al., 2005) and skeletal muscle (this report) development after α-actinin levels plateaued, suggesting that low N-RAP levels are sufficient to catalyze myofibril assembly but that larger reserves of N-RAP accumulate at the ends of the myofibrils in the mature tissue.

Some studies on myofibril assembly in precardiac mesoderm explant cultures (Rudy et al., 2001) and embryonic hearts (Ehler et al., 1999) have suggested that important features of the process observed in isolated cultured cells do not reflect the mechanism of assembly in the intact tissue; these studies emphasized the absence of premyofibrils containing nonmuscle myosin and short sarcomeres to suggest that the mechanism of myofibril assembly observed in culture systems may differ from what occurs in vivo (Ehler et al., 1999; Rudy et al., 2001). However, some earlier studies (e.g. (Imanaka-Yoshida, 1997) and recent data from Sanger and colleagues (Du et al., 2003; Du et al., 2008) convincingly demonstrate the presence of premyofibrils in cardiac organ culture, as well as in cultured skeletal muscle (Sanger et al., 2002). We also recently reported that premyofibril structures were present in embryonic mouse hearts but were much less prevalent than in spreading cultured cardiomyocytes, and proposed that this was due to the accumulation of assembly intermediates in cultured cells; we attributed this to the large pool of unassembled structural components present in the cultured cells versus the limited pool of scaffolding molecules needed for myofibril maturation (Lu et al., 2005). The implication was that different experimental systems share the same basic mechanism of myofibril assembly, although the kinetics of the various steps in assembly may be perturbed. Our finding that N-RAP is asscociated with similar assembling structures in the developing heart (Lu et al., 2005), cultured cardiomyocytes (Carroll and Horowits, 2000; Lu et al., 2003), developing skeletal muscle (figure 2), and differentiating myotubes (figure 6) is consistent with the view that the fundamental mechanism of myofibrillogenesis is the same in each case, and that N-RAP plays a role in the first steps of assembly.

N-RAP Alternative Splicing

Alternative splicing of N-RAP exon 12 is conserved between mice and humans, with expression of this exon found in skeletal muscle, but not in cardiac muscle, in both species (Mohiddin et al., 2003; Lu et al., 2005). Our results establish that N-RAP-s is the predominant spliced form of N-RAP throughout skeletal muscle development in the mouse. However, N-RAP alternative splicing was assessed using RNA isolated from a mixture of lower limb

muscles; therefore, any differences between fast and slow twitch fibers remains to be determined. Although the function of alternative splicing of the N-RAP gene is unknown, exon 12 encodes a single module in the simple repeat region of N-RAP. Binding partners for this region include α-actinin (Zhang et al., 2001; Lu et al., 2003), Krp1 (Lu et al., 2003), actin (Luo et al., 1999), and MLP (Ehler et al., 2001), and the presence of exon 12 could conceiveably affect the binding of any of these proteins.

Alternative splicing has long been recognized as a source of isoform diversity between tissues and developmental stages in muscle (Buckingham, 1989; Murphy, 1996). Even though the functional consequences of this diversity have not always been apparent, recent work has shown that defects in alternative splicing can account for many of the clinical features in myotonic dystrophy (Cho and Tapscott, 2007; Wheeler and Thornton, 2007). In this muscle disease, expression of RNA containing aberrant CUG repeats leads to sequestering of MBNL1, a member of the muscleblind-like (MBNL) family of splicing factors, in nuclear foci (Cho and Tapscott, 2007; Wheeler and Thornton, 2007). Genetic mouse models of myotonic dystrophy include transgenic expression of CUG repeats and MBNL1 knockouts, and each of these models exhibits a specific failure of post-natal alternative splicing transitions in a wide variety of genes, including N-RAP (Lin et al., 2006). Unlike normal adult skeletal muscle in which N-RAP-s is predominant, the proportion of N-RAP-c messages is aberrantly increased in muscle from myotonic dystrophy patients or mice (Lin et al., 2006). Exploring functional differences between N-RAP isoforms will be important for determining if aberrant N-RAP splicing plays any role in the muscle pathology of myotonic dystrophy.

Acknowledgments

This research was supported by the Intramural Research Program of the National Institute of Arthritis and Musculoskeletal and Skin Diseases of the National Institutes of Health (NIH) and by an intramural Uniformed Services University of the Health Sciences grant to D.E.B. We thank Drs. Evelyn Ralston and Kristien Zaal (Light Imaging Section, NIAMS) for instruction and guidance with the confocal microscopy.

Grant Sponsor: Uniformed Services University of the Health Sciences; Grant number CO70VY

References

Buckingham ME. The control of muscle gene expression: a review of molecular studies on the production and processing of primary transcripts. Br Med Bull 1989;45:608–629. [PubMed: 2688820]

Carroll S, Lu S, Herrera AH, Horowits R. N-RAP scaffolds I-Z-I assembly during myofibrillogenesis in cultured chick cardiomyocytes. J Cell Sci 2004;117:105–114. [PubMed: 14657273]

Carroll SL, Herrera AH, Horowits R. Targeting and functional role of N-RAP, a nebulin-related LIM protein, during myofibril assembly in cultured chick cardiomyocytes. J Cell Sci 2001;114:4229–4238. [PubMed: 11739655]

Carroll SL, Horowits R. Myofibrillogenesis and formation of cell contacts mediate the localization of N-RAP in cultured chick cardiomyocytes. Cell Motil Cytoskeleton 2000;47:63–76. [PubMed: 11002311]

Cho DH, Tapscott SJ. Myotonic dystrophy: emerging mechanisms for DM1 and DM2. Biochim Biophys Acta 2007;1772:195–204. [PubMed: 16876389]

Dabiri GA, Turnacioglu KK, Sanger JM, Sanger JW. Myofibrillogenesis visualized in living embryonic cardiomyocytes. Proc Natl Acad Sci U S A 1997;94:9493–9498. [PubMed: 9256510]

Dhume A, Lu S, Horowits R. Targeted disruption of N-RAP gene function by RNA interference: A role for N-RAP in myofibril organization. Cell Motil Cytoskeleton 2006;63:493–511. [PubMed: 16767749]

Dlugosz AA, Antin PB, Nachmias VT, Holtzer H. The relationship between stress fiber-like structures and nascent myofibrils in cultured cardiac myocytes. J Cell Biol 1984;99:2268–2278. [PubMed: 6438115]

Du A, Sanger JM, Linask KK, Sanger JW. Myofibrillogenesis in the first cardiomyocytes formed from isolated quail precardiac mesoderm. Dev Biol 2003;257:382–394. [PubMed: 12729566]

Du A, Sanger JM, Sanger JW. Cardiac myofibrillogenesis inside intact embryonic hearts. Dev Biol 2008;318:236–246. [PubMed: 18455713]

Ehler E, Horowits R, Zuppinger C, Price RL, Perriard E, Leu M, Caroni P, Sussman M, Eppenberger HM, Perriard JC. Alterations at the intercalated disk associated with the absence of muscle LIM protein. J Cell Biol 2001;153:763–772. [PubMed: 11352937]

Ehler E, Rothen BM, Hämmerle SP, Komiyama M, Perriard JC. Myofibrillogenesis in the developing chicken heart: assembly of the z-disk, m-line and thick filaments. Journal of Cell Science 1999;112:1529–1539. [PubMed: 10212147]

Gehmlich K, Geier C, Osterziel KJ, Van Der Ven PF, Furst DO. Decreased interactions of mutant muscle LIM protein (MLP) with N-RAP and alpha-actinin and their implication for hypertrophic cardiomyopathy. Cell Tissue Res 2004;317:129–136. [PubMed: 15205937]

Giulietti A, Overbergh L, Valckx D, Decallonne B, Bouillon R, Mathieu C. An overview of real-time quantitative PCR: applications to quantify cytokine gene expression. Methods 2001;25:386–401. [PubMed: 11846608]

Greenberg CC, Connelly PS, Daniels MP, Horowits R. Krp1 (Sarcosin) promotes lateral fusion of myofibril assembly intermediates in cultured mouse cardiomyocytes. Exp Cell Res 2008;314:1177–1191. [PubMed: 18178185]

Gregorio CC, Antin PB. To the heart of myofibril assembly. Trends Cell Biol 2000;10:355–362. [PubMed: 10932092]

Handel SE, Greaser ML, Schultz E, Wang SM, Bulinski JC, Lin JJ, Lessard JL. Chicken cardiac myofibrillogenesis studied with antibodies specific for titin and the muscle and nonmuscle isoforms of actin and tropomyosin. Cell Tissue Res 1991;263:419–430. [PubMed: 1878931]

Holtzer H, Hijikata T, Lin ZX, Zhang ZQ, Holtzer S, Protasi F, Franzini-Armstrong C, Sweeney HL. Independent assembly of 1.6 microns long bipolar MHC filaments and I-Z- I bodies. Cell Struct Funct 1997;22:83–93. [PubMed: 9113394]

Imanaka-Yoshida K. Myofibrillogenesis in precardiac mesoderm explant culture. Cell Struct Funct 1997;22:45–49. [PubMed: 9113389]

Lin X, Miller JW, Mankodi A, Kanadia RN, Yuan Y, Moxley RT, Swanson MS, Thornton CA. Failure of MBNL1-dependent post-natal splicing transitions in myotonic dystrophy. Hum Mol Genet 2006;15:2087–2097. [PubMed: 16717059]

Livak KJ, Schmittgen TD. Analysis of relative gene expression data using real-time quantitative PCR and the 2(-Delta Delta C(T)) Method. Methods 2001;25:402–408. [PubMed: 11846609]

Lu S, Borst DE, Horowits R. N-RAP expression during mouse heart development. Dev Dyn 2005;233:201–212. [PubMed: 15765519]

Lu S, Carroll SL, Herrera AH, Ozanne B, Horowits R. New N-RAP-binding partners α-actinin, filamin and Krp1 detected by yeast two-hybrid screening: implications for myofibril assembly. J Cell Sci 2003;116:2169–2178. [PubMed: 12692149]

Luo G, Herrera AH, Horowits R. Molecular interactions of N-RAP, a nebulin-related protein of striated muscle myotendon junctions and intercalated disks. Biochemistry 1999;38:6135–6143. [PubMed: 10320340]

Luo G, Zhang JQ, Nguyen TP, Herrera AH, Paterson B, Horowits R. Complete cDNA sequence and tissue localization of N-RAP, a novel nebulin-related protein of striated muscle. Cell Motil Cytoskeleton 1997;38:75–90. [PubMed: 9295142]

Mohiddin SA, Lu S, Cardoso JP, Carroll SL, Jha S, Horowits R, Fananapazir L. Genomic organization, alternative splicing, and expression of human and mouse N-RAP, a nebulin-related LIM protein of striated muscle. Cell Motil Cytoskeleton 2003;55:200–212. [PubMed: 12789664]

Murphy AM. Contractile protein phenotypic variation during development. Cardiovasc Res 1996;31:Spec No:E25–33.

Rhee D, Sanger JM, Sanger JW. The premyofibril: evidence for its role in myofibrillogenesis. Cell Motil Cytoskeleton 1994;28:1–24. [PubMed: 8044846]

Rudy DE, Yatskievych TA, Antin PB, Gregorio CC. Assembly of thick, thin, and titin filaments in chick precardiac explants. Dev Dyn 2001;221:61–71. [PubMed: 11357194]

Sanger JW, Chowrashi P, Shaner NC, Spalthoff S, Wang J, Freeman NL, Sanger JM. Myofibrillogenesis in skeletal muscle cells. Clinical Orthopaedics & Related Research 2002;403:S153–162. [PubMed: 12394464]

Sanger JW, Kang S, Siebrands CC, Freeman N, Du A, Wang J, Stout AL, Sanger JM. How to build a myofibril. J Muscle Res Cell Motil 2005;26:343–354. [PubMed: 16465476]

Schultheiss T, Lin ZX, Lu MH, Murray J, Fischman DA, Weber K, Masaki T, Imamura M, Holtzer H. Differential distribution of subsets of myofibrillar proteins in cardiac nonstriated and striated myofibrils. J Cell Biol 1990;110:1159–1172. [PubMed: 2108970]

Srikakulam R, Winkelmann DA. Chaperone-mediated folding and assembly of myosin in striated muscle. J Cell Sci 2004;117:641–652. [PubMed: 14709723]

Wang SM, Greaser ML, Schultz E, Bulinski JC, Lin JJ, Lessard JL. Studies on cardiac myofibrillogenesis with antibodies to titin, actin, tropomyosin, and myosin. J Cell Biol 1988;107:1075–1083. [PubMed: 3047149]

Wheeler TM, Thornton CA. Myotonic dystrophy: RNA-mediated muscle disease. Curr Opin Neurol 2007;20:572–576. [PubMed: 17885447]

Zhang JQ, Elzey B, Williams G, Lu S, Law DJ, Horowits R. Ultrastructural and biochemical localization of N-RAP at the interface between myofibrils and intercalated disks in the mouse heart. Biochemistry 2001;40:14898–14906. [PubMed: 11732910]

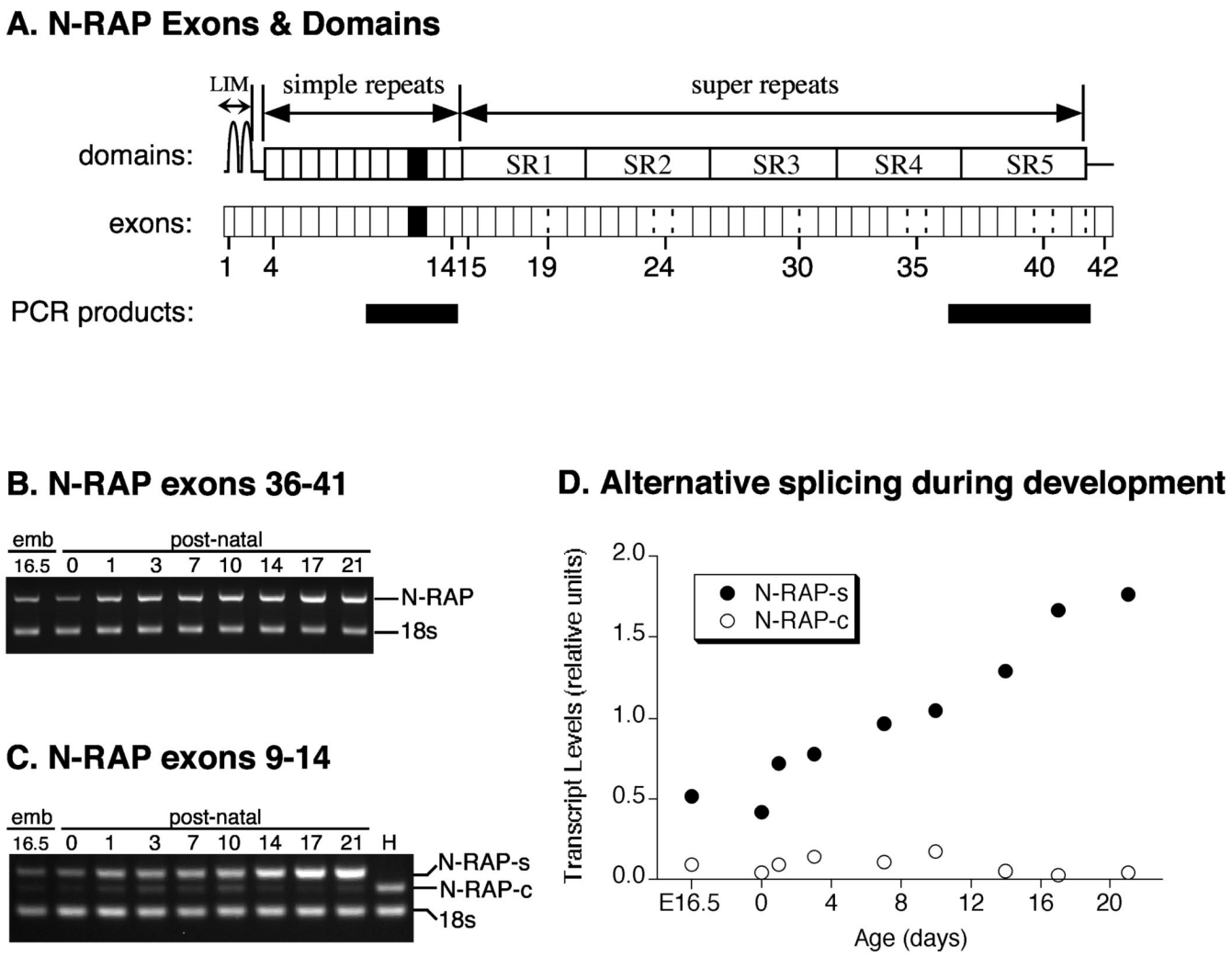

Figure 1.

(A) N-RAP domain organization and corresponding exons (Mohiddin et al., 2003). Exons 1 and 2 together encode a LIM domain; exons 4-14 encode single repeating modules; and exons 15-41 encode 5 super repeats, each of which contains 7 single modules. Exon boundaries correspond to module boundaries, except where dashed vertical lines indicate multiple modules encoded by a single exon. Exon 12 is alternatively spliced (filled box). The location of PCR products is illustrated below the domain and exon maps. (B-C) N-RAP PCR products amplified from cDNA made from RNA isolated from mouse skeletal muscle tissue. Numbers above the gels refer to embryonic or post-natal days of development, as indicated, where post-natal day 0 is the day of birth. N-RAP exons 9-14 were also amplified from mouse heart cDNA for comparison (panel C, lane H). N-RAP-s and N-RAP-c refer to isoforms containing or omitting N-RAP exon 12. 18s rRNA was amplified as an internal control. (D) Relative levels of N-RAP-s and N-RAP-c during skeletal muscle development. The results represent analysis of the band intensities in panel C and are normalized to the internal 18s controls.

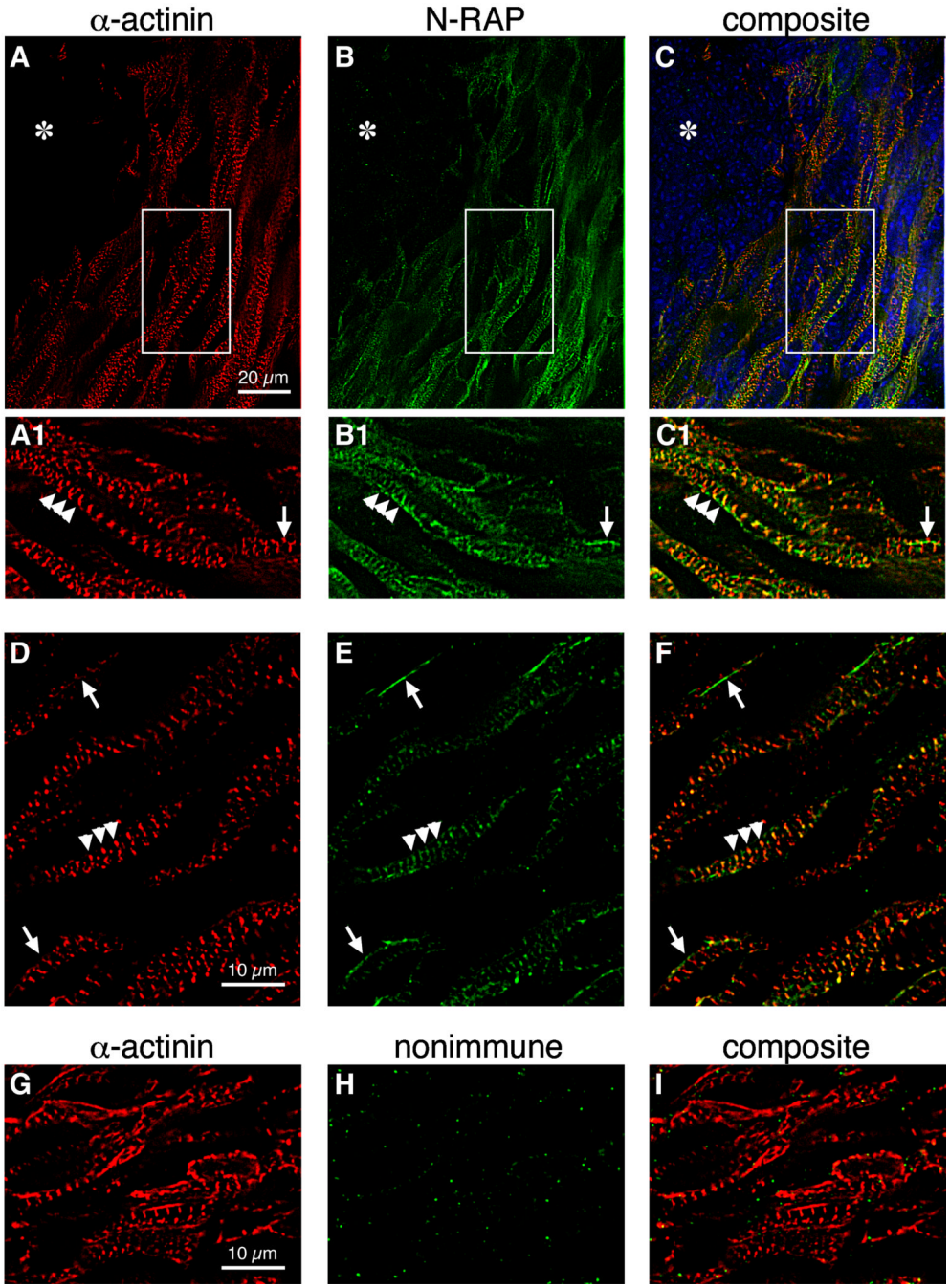

Figure 2.

Localization of α-actinin (red) and N-RAP (green) (A-F) or α-actinin (red) and the nonimmune control (green) (G-I) in skeletal muscle regions of E14.5 embryos. Dapi staining (blue, panel C) reveals nuclei of nonmuscle cells that are unlabeled by the antibodies (asterisks, A-C). The boxed regions in A-C are shown enlarged 2-fold below the main panels (A1-C1). Myofibrils marked by periodic bands of α-actinin (arrowheads), as well as closely spaced dots or narrow bands of α-actinin typical of myofibril precursors (arrows), are present (A1, D, G). N-RAP staining associated with myofibril precursors appears as a punctate or continuous line (arrows, B1, E), while N-RAP in more mature myofibrils stains at twice the α-actinin periodicity

(arrowheads, B1, E). Nonspecific punctate staining is evident with the nonimmune serum at this stage, but the nonspecific staining is not correlated with α-actinin staining (G-I).

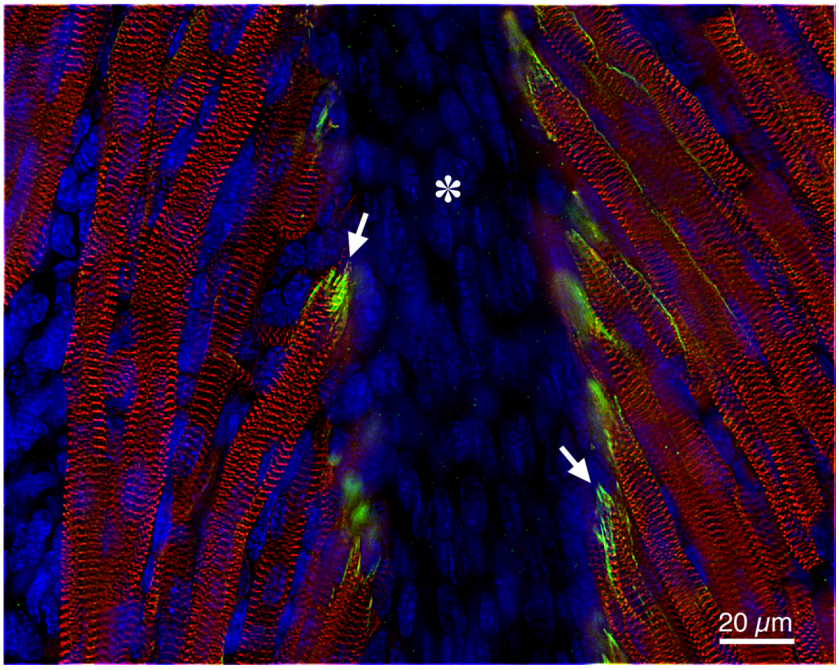

Figure 3.
Localization of α-actinin (red), N-RAP (green), and Dapi-stained nuclei (blue) in the limb region of an E17.5 embryo. N-RAP is concentrated in the myotendinous junction regions of mature myotubes (arrows), which connect to cartilage or bone running vertically through the image (asterisk).

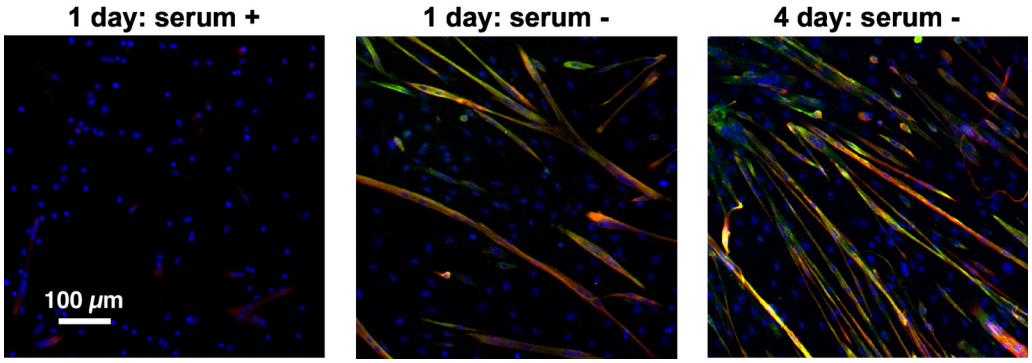

Figure 4.

Primary cultures of skeletal muscle labeled with antibodies against sarcomeric α-actinin (red) and N-RAP (green), and nuclei stained with Dapi (blue). Cells were cultured for the indicated times in medium containing normal (left panel) or reduced (center and right panels) serum. Serum withdrawal is accompanied by myoblast differentiation and fusion to form myotubes.

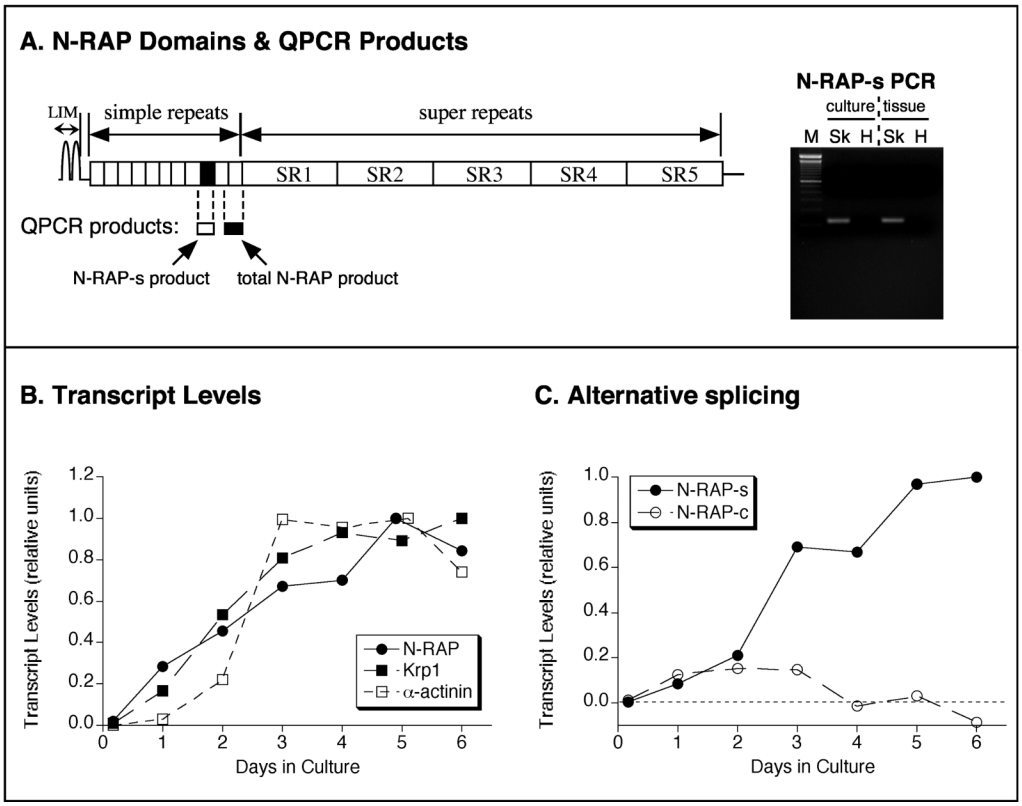

Figure 5.

Real-time PCR analysis of transcript levels in differentiating primary cultured skeletal muscle. (A) N-RAP domain organization showing the position of PCR products designed to measure N-RAP-s and total levels of N-RAP. The specificity of N-RAP-s detection is illustrated in the gel photo at the right for both skeletal muscle cultures and tissue (M, size markers; Sk, skeletal muscle; H, heart). (B) Time-course of muscle-specific transcript accumulation during culture in differentiation medium. Transcript levels were normalized to 18S rRNA levels in the same samples, and then scaled so that the maximum level of each mRNA measured during the experiment was 1. (C) N-RAP isoform transcripts during culture in differentiation medium. N-RAP-s and total N-RAP transcript levels were measured by real-time PCR of the regions indicated in panel A, and N-RAP-c levels were calculated as the difference between the two.

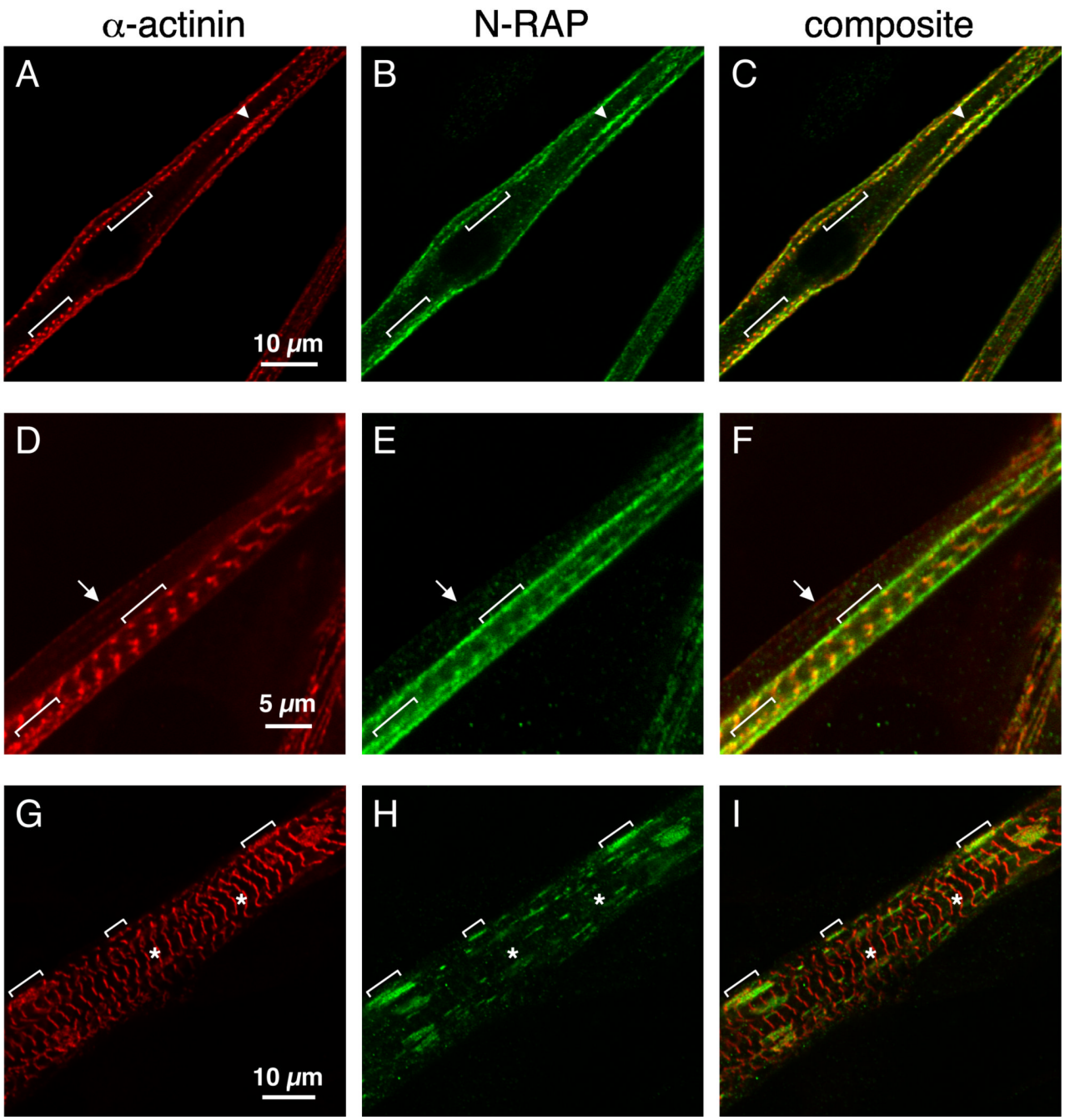

Figure 6.
Confocal imaging of α-actinin (red) and N-RAP (green) staining in cultured primary myotubes. N-RAP is concentrated in premyofibril structures containing closely spaced dots of α-actinin (A-I, arrowhead and brackets), but is not present in mature sarcomeres (G-I, asterisks) or at the spreading lateral edge of cells (D-F, arrow).

Table 1

PCR Primer Pairs

Amplified mRNA	Primer Pair	Product Size
N-RAP, exons 9-14	Forward: 5′-GACCGATGTGGCCAGGTTTACTCAGAAG-3′ Reverse: 5′-CAGGGGAACCAGCCTCATCGTTGTTTG-3′	549 bp (N-RAP-s) 444 bp (N-RAP-c)
N-RAP, exons 36-41	Forward: 5′-TGATGGGCATGAAAGGGACAGGAT-3′ Reverse: 5′-ATCCCCGGGCCCCTCCTGTT-3′	829 bp
Total N-RAP	Forward: 5′-TGCTCCACGCTCTCAAAGTTGG-3′ Reverse: 5′-TGACATCCTTCAGGGGAACCAG-3′	147 bp
N-RAP-s	Forward: 5′-AGCTTGTGAGTGAGGTGGAGTA-3′ Reverse: 5′-CGCTGGTGAATTTTGAGATCTTG-3′	117 bp
α-actinin (2 + 3)	Forward: 5′-ATCATCCTCCGCTTCGCCATTC-3′ Reverse: 5′-TCTTCAGCATCCAACATCTTAGG-3′	290 bp
Krp1	Forward: 5′-AATGGGCTGGGATGCTGAAG-3′ Reverse: 5′-CACCTTGGGGATTCGGTTACAC-3′	249 bp

PCR primers used to amplify the indicated products. Primers used to amplify N-RAP exons 9-14 or exons 36-41 were used for semi-quantitative RT-PCR. All other primer pairs were used in quantitative real-time PCR assays.